Biosensors and Bioelectronics 26 (2010) 760–765

Contents lists available at ScienceDirect

Biosensors and Bioelectronics

journal homepage: www.elsevier.com/locate/bios

Imprinting of protein over silica nanoparticles via surface graft copolymerization using low monomer concentration

Hongyan He, Guoqi Fu*, Yan Wang, Zhihua Chai, Yizhe Jiang, Zilun Chen

Key Laboratory of Functional Polymer Materials of Ministry of Education, Institute of Polymer Chemistry, Nankai University, No. 94 Weijin Road, Tianjin 300071, PR China

ARTICLE INFO

Article history:
Received 23 March 2010
Received in revised form 6 June 2010
Accepted 24 June 2010
Available online 3 July 2010

Keywords:
Molecular imprinting
Protein imprinting
Surface imprinting
Nanoparticles
Lysozyme

ABSTRACT

Surface imprinting and adopting a nano-sized physical form are two effective approaches to overcome the template transfer difficulty within molecularly imprinted polymers and in particular advantageous to the imprinting of macromolecular structures like proteins. The surface protein-imprinted nanoparticles based on these two strategies are attractive for biosensor development. We here demonstrate a facile way for imprinting protein over nanoparticle supports. It was achieved simply via radical induced graft copolymerization of low concentration monomers on the surface of vinyl modified silica nanoparticles dispersed in aqueous media with lysozyme as a model protein. With a total monomer concentration of 0.4 wt%, less than tenth that employed conventionally, the possible gelation of the dispersion after polymerization was avoided and hence the unagglomerated imprinted particles could be readily collected. It was proved that thin polymer shells with imprinted sites had been formed over the support particles. In batch rebinding tests, the imprinted particles reached saturated adsorption within 5 min and exhibited significant specific recognition toward the template protein. The presented approach may be a versatile way for the fabrication of surface protein-imprinted nanoparticles via rational design of the surface chemistry of the support particles and choice of functional monomers according to the properties of the print protein.

1. Introduction

There is a great need for the synthetic materials with molecular recognition ability for biomacromolecules such as proteins. These affinity materials can find important applications in the areas of biosensors (Tai et al., 2010), separation (Zhao et al., 2006), medical diagnostics (Wang et al., 2010) and drug delivery (Bergmann and Peppas, 2008). Antibodies are usually used for these purposes. However, they are too expensive and unstable, and hence synthetic materials for selective protein recognition have attracted increasing research interest.

Molecular imprinting is an inexpensive method for the synthesis of tailor-made recognition materials by copolymerizing suitable functional monomers in the presence of desired template molecules. Compared with natural recognition materials, e.g. antibodies, molecularly imprinted polymers (MIPs) offer advantages like stability, specific recognition and ease of mass preparation, and thus have been applied in wide areas including separation, catalysis and sensors (Haupt and Mosbach, 2000; Marty and Mauzac, 2005; Bergmann and Peppas, 2008). To date, the molecular imprinting technology against small molecules has been well-established. However, the imprinting of proteins and other biomacromolecules continues to be a significant challenge. The major problem lies in their restricted mass transfer across the cross-linked polymer matrix due to the large molecular sizes, which restricts the ease of template removal as well as rebinding. Other problems include complex and flexible structures of proteins, and significantly reduced non-covalent template–monomer interactions in aqueous media where proteins prefer to exist (Hawkin et al., 2005; Shiomi et al., 2005; Li et al., 2006). Considering these difficulties, a variety of approaches have been developed, for example, surface imprinting (Bossi et al., 2001; Shiomi et al., 2005), epitope imprinting (Rachkov and Minoura, 2001; Nishino et al., 2006), and the use of novel materials such as sol–gel derived xerogels (Lee et al., 2007) and moderately cross-linked hydrogels (Hawkin et al., 2005) including stimuli-responsive hydrogels (Hua et al., 2008) and supermacroporous cryogels (Bereli et al., 2008). The advances in this field have been reviewed comprehensively (Turner et al., 2006; Bossi et al., 2007; Hansen, 2007; Janiak and Kofinas, 2007; Ye and Mosbach, 2008). However, new approaches for protein imprinting are still highly desired, especially those which are widely applicable and easy to perform.

Nanostructured MIPs have a small dimension with extremely high surface-to-volume ratio, so that most of template molecules are situated at the surface or in the proximity of the material's sur-

* Corresponding author. Tel.: +86 22 23501443; fax: +86 22 23501443.
E-mail address: gqfu@nankai.edu.cn (G. Fu).

0956-5663/$ – see front matter © 2010 Elsevier B.V. All rights reserved.
doi:10.1016/j.bios.2010.06.043

face (Gao et al., 2007). Obviously, nano-sized MIPs are expected to improve the binding capacity, binding kinetics and accessibility of the recognition sites generated. Recently, several research groups have begun to explore different nanotechniques for the imprinting of protein molecules. The reported strategies include the use of porous alumina as a sacrificial nanomold to fabricate imprinted nanowires (Li et al., 2006) or surface-bound nanofilaments (Linares et al., 2009), oxidization of 3-aminophenylboronic acid (Li et al., 2009) or dopamine (Zhou et al., 2010) to form imprinted coatings over magnetic nanoparticles, facile formation of protein-imprinted poly(ethylene-co-vinyl alcohol)/quantum dot composite nanoparticles via phase inversion of the polymer (Lin et al., 2009) and the synthesis of imprinted nanoparticles via aqueous solution precipitation polymerization (Cutivet et al., 2009; Hoshino et al., 2008). Shea and coworkers (Hoshino et al., 2008) synthesized peptide-imprinted polymer nanoparticles via aqueous solution precipitation polymerization below 25 °C in the presence of very low concentrations of surfactant. N-isopropylacrylamide (NIPAm) was used as the backbone monomer in combination with other functional monomers, in particular hydrophobic N-*tert*-butylacrylamide (TBAm) to decrease the volume phase transition temperature of the resultant copolymers. Haupt and coworkers (Cutivet et al., 2009) synthesized trypsin-imprinted nanoparticles by surfactant-free precipitation polymerization under high dilution conditions. Acrylamide and another strong anchoring monomer were copolymerized in aqueous media with a high cross-linking degree up to 60%. Among the reported approaches for the synthesis of nano-sized protein-imprinted polymers, these based on precipitation polymerization may be more versatile, since various (methyl)acrylic functional monomers can be chosen according to the properties of the protein to be imprinted. However, the size of the imprinted particles strongly depended on the prepolymerization recipes, as observed with conventional precipitation polymerization. Also, most of the recognition sites generated would be inside the nanoparticles, with a greatly reduced accessibility compared to the surface-imprinted particles. The mass transfer limitation may be more pronounced in the case of highly cross-linked particles.

In this report, we demonstrate the feasibility of an alternative approach for producing surface-imprinted nanoparticles for protein recognition. With vinyl modified nanoparticles as supports, surface graft copolymerization of (meth)acrylic functional and cross-linking monomers is let to occur in aqueous solutions, which are dilute enough to avoid the possible gelation of the reaction dispersion. The core–shell structure of the resultant imprinted particles can facilitate template removal and rebinding. The size of the imprinted particles principally depends on that of the original supports. Additionally, different functions other than molecular imprinting may be readily incorporated into the imprinted particles simply by using other vinyl modified nanocores with desired properties, such as magnetic nanoparticles, colloidal gold or silver particles and quantum dot nanocrystals. For the experimental proof of concept, lysozyme was imprinted over the vinyl modified silica nanoparticles via surface graft copolymerization of acrylamide combined with other two oppositely charged monomers and a cross-linker in dilute aqueous solutions, according to the prepolymerization recipes for the synthesis of lysozyme-imprinted hydrogels reported previously (Ou et al., 2004; Kimhi and Bianco-Peled, 2007). The resultant surface-imprinted particles were characterized by transmission electron microscopy (TEM), thermogravimetric analysis (TGA) and X-ray photoelectron spectroscopy (XPS). The protein adsorption characteristics of the particles were examined by batch rebinding tests, competitive batch rebinding tests and rebinding kinetics study.

2. Experimental

2.1. Materials

Tetraethylorthosilicate (TEOS) and methacrylic acid (MAA) were provided by Tianjin Chemical Reagents Co., Ltd. (Tianjin, China) and distillated under reduced pressure before use. 3-Methacryloxypropyl trimethoxysilane (MPS) was purchased from Diamond Advanced Materials Inc. (Hubei, China). 2-(Dimethylamino)ethyl methacrylate (DMAEMA) was purchased from Aldrich and passed through a basic Al_2O_3 column for the removal of polymerization inhibitor. Acrylamide (AAm) and N,N′-methylenebisacrylamide (MBA) of electrophoresis grade, lysozyme (Lys), bovine serum albumin (BSA) were obtained from Dingguo Biotech Co., Ltd. (Beijing, China). Cytochrome c (Cyt c) was purchased from Sangon (Shanghai, China). Bovine hemoglobin (Hb) and ribonuclease A (RNase A) were purchased from Sigma. Ammonium persulfate (APS) and N,N,N′,N′-tetramethylethylenediamine (TEMED) of analytical grade were purchased from Tianjin Chemical Reagents Co., Ltd. All other chemicals were of analytical grade and used as received.

2.2. Preparation of vinyl modified silica nanoparticles

Monodisperse silica nanoparticles were synthesized according to the reported Stöber method (Stöber and Fink, 1968) and subsequently modified with MPS according the literature (Bourgeat-Lami and Lang, 1998). Briefly, 12 mL of TEOS was added to the mixture of 200 mL of ethanol, 22 mL of deionized water and 12 mL of aqueous solution of 25% ammonium with vigorous stirring at 30 °C and the reaction was continued overnight. To the resulting suspension, 1.5 mL of MPS diluted with 1.5 mL of ethanol was dropped in 0.5 h. Then the coating of the silica particles with MPS was achieved by stirring the mixture for 24 h. The resultant MPS-modified silica particles (denoted as MPS–Silica) were purified by three cycles of centrifugation, decantation, and resuspension in ethanol by ultrasonic. Finally, the product was freeze-dried to constant weight.

2.3. Preparation of surface Lys-imprinted nanoparticles

MBA (16 mg), AAm (32.6 mg, 0.458 mmol), MAA (39.4 mg, 0.458 mmol) and DMAEMA (72 mg, 0.458 mmol) were dissolved in 32 mL of phosphate buffer (pH 7.0, 0.02 mol/L) and mixed thoroughly by ultrasonic. To this solution, 32 mg of Lys was dissolved and then mixed with the suspension of MPS–Silica (120 mg) dispersed in 4 mL of ethanol and 4 mL of the phosphate buffer. After 1-h shaking for preassembly, the mixture was degassed under vacuum for 10 min and purged with nitrogen stream for another 10 min. By injecting 120 μL of APS solution (10%, w/w) and 60 μL of TEMED solution (5%, w/v) to the mixture, polymerization was initiated and continued under violent starring at 25 °C for 24 h. After the reaction, the Lys-imprinted particles were collected by centrifugation. The particles were washed with deionized water to remove adsorbed oligomers and unreacted monomers. They were then washed repeatedly with 0.5 M NaCl solution to remove embedded template until no Lys in the supernatant was detected using a UV/Vis spectrophotometer at 280 nm. Subsequently, they were re-washed with deionized water to remove remaining NaCl. Finally, the particles were equilibrated with the phosphate buffer and then freeze-dried for further use. The control non-imprinted particles were prepared and washed in the same way but without addition of the template. The imprinted and non-imprinted particles are denoted as Lys-MIP and NIP, respectively.

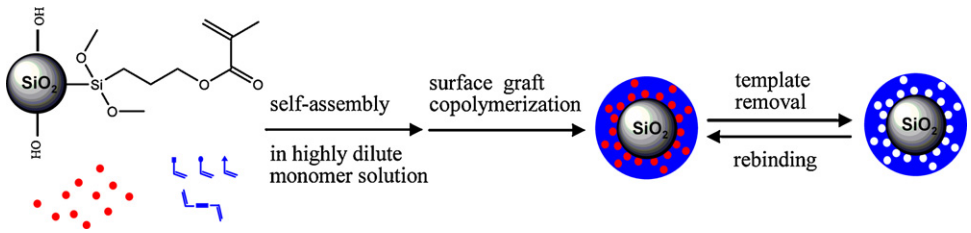

Fig. 1. Schematic illustration of the imprinting of Lys over MPS-modified silica nanoparticles via surface graft copolymerization in highly dilute solution of functional and cross-linking monomers. The possible gelation of the reaction mixture during the polymerization is avoided by adopting a sufficiently low monomer concentration and hence the resulting core–shell imprinted particles can be readily collected by centrifugation.

2.4. Batch rebinding tests

The nanoparticles weighed accurately (typically ~7.0 mg) were placed into a 2-mL centrifuge tube. The protein solutions at different initial concentrations were prepared in phosphate buffer (pH 7.0, 0.02 mol/L). Then 1.5 mL of each solution was added into the tube and thoroughly mixed with the contained particles by ultrasonic. The dispersion was allowed to incubate at 25 °C for 1 h. After centrifugation at 10,000 rpm for 5 min, the final concentration of the supernatant in the tube was determined by a UV/Vis spectrophotometer at 280 nm. The amount of protein adsorbed by the particles at the end of each run was calculated from the following formula:

$$Q = \frac{(C_i - C_f)V}{m}$$

where Q (mg/g) is the mass of protein adsorbed by unit mass of dry particles, C_i (mg/mL) and C_f (mg/mL) are the concentrations of the initial and final solutions, respectively, V (mL) is the total volume of the adsorption mixture, and m is the mass of the particles used. All the tests were conducted in triplicates.

2.5. Competitive batch rebinding tests

Cyt c was used as a competitive protein. The particles were subjected to a binary protein solution of Lys and Cyt c with individual initial concentrations of 0.2 mg/mL. The adsorption experiments were carried out similarly as the single-protein rebinding tests described in Section 2.4. The final concentration of both proteins in the supernatant was determined by a double-wavelength UV/Vis spectrophotometry and the determination wavelengths are selected as 280 and 410 nm.

2.6. Rebinding kinetics

The adsorption kinetics of the prepared particles was studied with an initial Lys concentration of 0.4 mg/mL. The adsorption runs were performed similarly to the single-protein batch rebinding tests except that a series of gradually increased adsorption times were employed.

2.7. Characterization

The morphologies and structures of the nanoparticles were examined by TEM (Tecnai G^2 20 S-TWIN, FEI). The samples for TEM were dispersed in ethanol and a drop of the dispersion was spread on amorphous carbon-coated 200 mesh copper grids, followed by drying at ambient temperature. TGA was carried out for the particle samples (~10 mg) using a NETZSCH TG 209 thermogravimetric analyzer under nitrogen atmosphere with a heating rate of 10 °C/min up to 800 °C. XPS was employed to determine the surface elementary composition of the particles. The XPS measurements were carried out on a Kratos AXIS HSi spectrometer equipped with a monochromatized Al KR X-ray source (1468.6 eV photos).

3. Results and discussion

3.1. Synthesis and characterization of Lys-imprinted silica nanoparticles

Previously, Ou et al. (2004) and Kimhi and Bianco-Peled (2007) studied Lys-imprinted hydrogels. They combined AAm with MAA and DMA as functional monomers, using MBA as a cross-linking monomer. The monomer ratio was optimized toward higher imprinting efficiency. According to these results, we chose Lys as print protein and employed the same monomer composition but with a much reduced concentration (from 20 to 0.4 wt%). Fig. 1 illustrates the procedure for the synthesis of surface Lys-imprinted silica nonoparticles. The MPS-modified colloidal silica particles are first mixed with the dilute solution of the monomers in the presence of Lys for self-assembly. After radical initiation of the polymerization, the possible gelation of the dispersion is avoided by adopting a very low total monomer concentration of 0.4 wt%. Nevertheless, the imprinted polymer shell-layers can be formed over the mod-

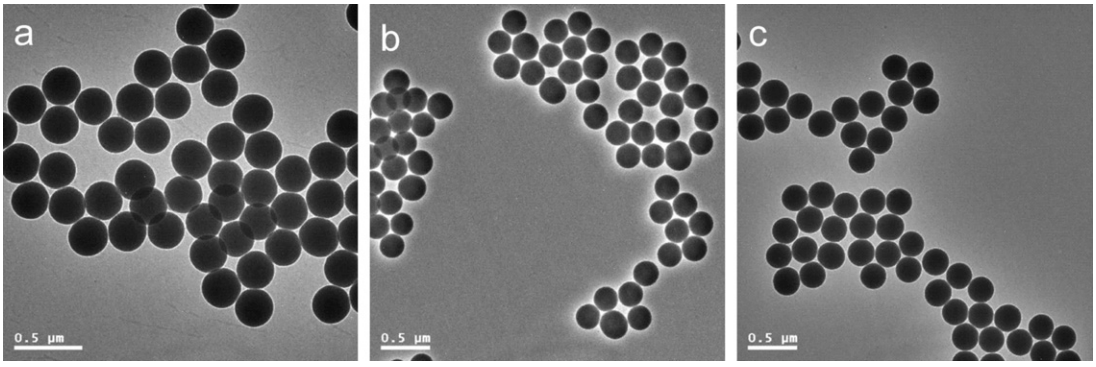

Fig. 2. TEM images of (a) Lys-imprinted particles, (b) non-imprinted particles and (c) MPS-modified silica particles.

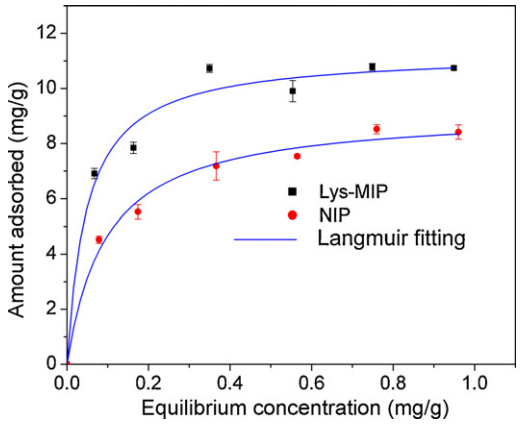

Fig. 3. Adsorption isotherms of Lys on the Lys-imprinted particles and non-imprinted particles. V = 1.5 mL, m = 7.0 mg, C_0 = 0.4–1.0 mg/g, time 1 h, temperature 25 °C, pH 7.0.

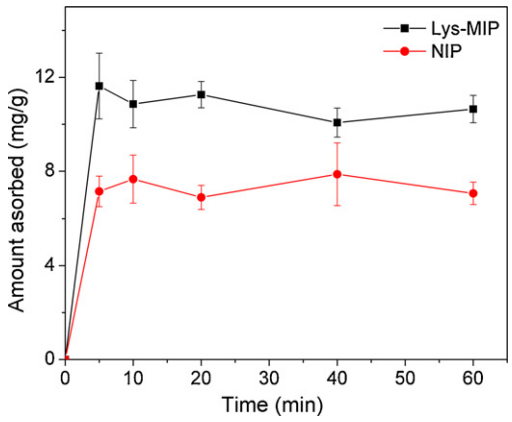

Fig. 4. Dynamic binding profiles of Lys on the Lys-imprinted and non-imprinted particles. V = 1.5 mL, m = 7.0 mg, C_0 = 0.4 mg/g, temperature 25 °C, pH 7.0.

ified silica supports. The reactive vinyl groups on the surface of MPS-modified silica cores may play an important role for the encapsulation of the polymer shells via the continual capture of the monomers and newly formed oligomers in the solution during the polymerization. The surface-imprinted particles with a core–shell structure are eventually obtained following the removal of the embedded templates.

The TEM image of the MPS–Silica particles (Fig. 2a) shows that the particles are uniform sphere-shaped and monodisperse with an average size of ~250 nm. After the polymerization for imprinting, the dispersion exhibited no noticeable gelation and therefore the MIP particles as well as the NIP particles could be readily collected by centrifugation at 8000 rpm. As seen from Fig. 2b and c, both the MIP and NIP particles are unagglomerated and remain the morphology like the MPS–Silica particles before the polymerization. The MIP and NIP particles show no discernable core–shell structure (the higher resolution TEM images gives the similar results and the images not shown), and no distinct size increase compared to the original MPS-modified silica nanoparticles. This suggests that the shell-layers possibly formed over the core particles would be very thin, especially in dry state. From the TGA results (see supporting information, Fig. S1), however, the MIP and NIP particles show ~3.5% more weight loss than the MPS–Silica upon heated to 800 °C. The XPS wide spectra of the different silica particles were obtained (see supporting information, Fig. S2). Compared with the spectrum of the MPS–Silica, the spectra of both MIP and the NIP particles exhibit a strong N1s signal, probably arising from the nitrogen-containing monomers (AAm, DMAEMA and MBA). The signals of Si2p and Si2s, which appear in the spectrum of the MPS–Silica, persist in the spectra of the MIP and NIP particles. This suggests that the thickness of the polymer shells, if present, would be less than the sampling depth of the XPS technique (~7.5 nm in an organic matrix) (Fu et al., 2007). Combining the TGA and XPS results, we can deduce that there were thin polymer coatings outside the MIP and NIP particles.

3.2. Rebinding capacity and kinetics

In characterizing the adsorption behaviors of the MIP and NIP particles, they were subjected to rebinding equilibrium and kinetics studies. Batch rebinding tests were performed at different initial concentrations of Lys, ranging from 0.1 to 1.0 mg/L. Fig. 3 shows the rebinding capacities to Lys at different equilibrium concentrations, i.e. adsorption isotherms. Within the concentration range covered, the MIP particles exhibited much higher binding amounts than the control NIP particles and both of them tend to reach an adsorption plateau. This observation suggests that the molecular recognition sites were generated on the surface of the MIP particles by the Lys template involved in the polymerization process, considering no significant difference in morphology and other aspects between the MIP particles and the corresponding controls. The Langmuir model was used to describe the experimental data, which is expressed as:

$$q_e = \frac{q_m C_e}{K_d + C_e}$$

where C_e (mg/mL) is the equilibrium concentration of Lys in bulk solution, q_e (mg/g) the amount of adsorbed Lys on per gram of the MIP or NIP particles at the equilibrium concentration, q_m (mg/g) the saturation capacity and K_d (mg/mL) the dissociate constant. Nonlinear fitting of the data to the Langmuir equation yielded a good fit for the MIP and NIP particles (with the regression coefficient higher than 0.98), allowing to determine the parameters involved. The estimated q_m and K_d are 11.3 ± 0.4 mg/g and 0.049 ± 0.012 mg/mL for the MIP particles, and 9.2 ± 0.3 mg/g and 0.096 ± 0.015 mg/mL for the NIP particles, respectively. The lower K_d for the MIP particles corresponds to their higher affinity toward Lys molecules.

The rate of rebinding was further studied, for it is one of the important considerations for the practical application of the MIP particles. The experiments were performed with an initial Lys concentration of 0.4 mg/mL. As shown in Fig. 4, both the MIP and NIP particles reached the maximum adsorption within 5 min. The rebinding kinetics might be rapider than measured, since the shorter rebinding time was not adopted due to the experimental difficulties. The rebinding rate of our imprinted particles is exceedingly rapid, considering that the protein-imprinted nanoparticles reported previously often required more than 1 h for achieving the adsorption plateau (Li et al., 2009; Kan et al., 2010; Zhang et al., 2010). This surprisingly fast kinetics is consistent with the super-thin coating coatings created over the silica nanoparticles. With such fast rebinding character, the MIP particles obtained in this study may be particularly suitable for the application as a sensor recognition element. For this purpose, the imprinted nanoparticles can be used as a basic building block to assemble a recognition layer on the surface of a transducer like quartz crystal microbalance, either through immobilization in a thin polymer layer deposited on a transducer surface (Reimhult et al., 2008) or by a vertical deposition method to form colloidal crystal (Hu et al., 2007).

3.3. Rebinding specificity

In addition to the template Lys, four other proteins with different isoelectric points (pI) and molecular weights (MW) were chosen as

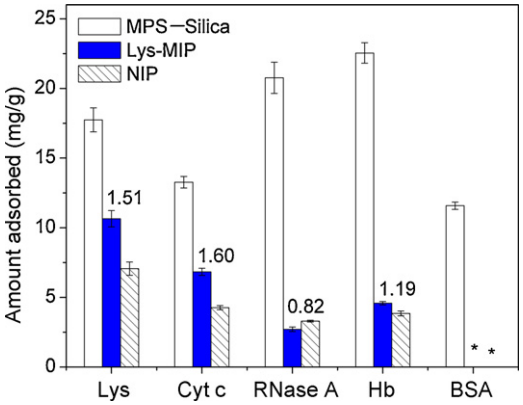

Fig. 5. Binding amounts of different proteins on the imprinted, non-imprinted and MPS-modified silica particles. V = 1.5 mL, m = 7.0 mg, C_0 = 0.4 mg/g, time 1 h, temperature 25 °C, pH 7.0. The imprinting factors are indicated above the bars. * denotes too little to be detected.

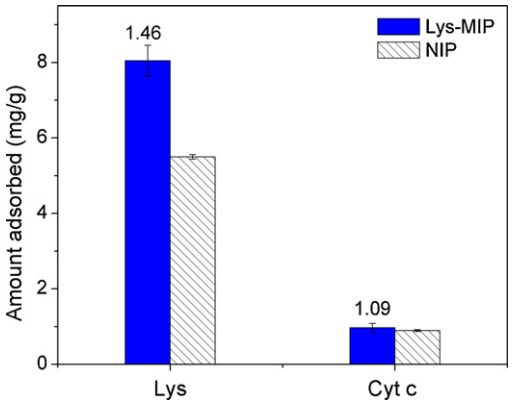

Fig. 6. Competitive binding of Lys and Cyt c to the imprinted, non-imprinted particles. V = 1.5 mL, m = 7.0 mg, $C_{0,Lys} = C_{0,Cyt\,c}$ = 0.2 mg/g, time 1 h, temperature 25 °C, pH 7.0. The imprinting factors are indicated above the bars.

references to study the selectivity of the MIP particles. The pI and MW of all the proteins studied are Lys (MW 1.4k, pI 11.1), Cyt c (MW 12.4k, pI 10.2), RNase A (MW 13.7k, pI 9.6), Hb (MW 64.5k, pI 6.8) and BSA (MW 66k, pI4.8). Fig. 5 shows the adsorption capacities of the MIP and NIP particles along with MPS–Silica particles for these proteins in pH 7.0 buffered solutions with a feed concentration of 0.4 mg/mL. Compared with both MIP and NIP particles, the MPS–Silica particles exhibited much higher binding amounts for all the proteins, resulting from the nonspecific interactions with the remaining silanol groups on the particles' surface. On the other hand, apart from the XPS and TGA results described in the Section 3.1, the greatly decreased capacities of the MIP and NIP particles further confirm the generation of thin polymer coatings over the MPS–Silica particles after the polymerization. The imprinting effect of a MIP is often evaluated by imprinting factor (IF) and specific adsorption capacity, with the former defined as the ratio of binding capacity of the MIP with respect to that of the NIP and the latter defined as the corresponding difference. The MIP particles exhibited significant adsorption selectivity for Lys with an IF of 1.51 and a specific rebinding of 3.58 mg/g. The BAS rebinding on both the MIP and NIP particles was too little to be detected, probably since that these particles were negatively charged as BSA molecules at pH 7.0. For Hb with a neutral pI and much higher MW than Lys, the MIP particles showed both lower IF and specific rebinding. RNase A and Cyt c have MW and pI rather close to these of Lys. Hence, the use of such similar proteins as references presents a genuine challenge to the imprinting process, since both the size of cavities and the nature of physical forces responsible for the recognition are supposed to be approximately same. The MIP particles showed no preference to RNase A with an IF of 0.82. A slightly higher IF of 1.60 was observed for Cyt c, however, the specific adsorption capacity for Cyt c was calculated to be 2.56 mg/g, quite lower than that for Lys (3.58 mg/g).

To further illustrate the recognition property of the MIP particles, binary protein competitive adsorption experiments were performed with Cyt c as the competitor. As shown in Fig. 6, whether from the point of IF or specific adsorption capacity, the MIP particles exhibited significant adsorption selectivity for the template Lys against Cyt c.

Compared with the granulated Lys-imprinted hydrogels based on the same functional and cross-linking monomers (Kimhi and Bianco-Peled, 2007), the Lys-imprinted nanoparticles in this study showed a comparative IF, but a greatly lower specific rebinding capacity against that of 36 mg/g of polymer. If the rebinding amount was also calculated in terms of the mass of the polymer shells (accounting for ~3.5 wt% of the core–shell particles), however, the Lys-imprinted nanoparticles in this work would give more than twice specific rebinding than that of the imprinted hydrogels. This can be principally attributed to the advantages of the nano-sized MIP (Gao et al., 2007). Additionally, the remaining silanol groups on the surface of the MPS-modified silica cores might play a role by enrichment of the templates from the prepolymerization solution before polymerization and co-operation with the functional and cross-linking monomers to create the imprinting sites while polymerization. With this conception in mind, the imprinting effect may be enhanced by special design of the surface chemistry of the core particles according to the properties of the template molecules.

4. Conclusions

Using Lys as a model protein, we have successfully demonstrated a new strategy for producing surface protein-imprinted nanoparticles by copolymerization of functional and cross-linking monomers on the surface of vinyl modified silica nanoparticles dispersed in dilute aqueous media in the presence of template protein. With highly dilute monomer concentration, the thin imprinted shells were generated over the support particles and the resulting imprinted particles remained separate and could be readily collected after polymerization. The imprinted particles showed fast adsorption kinetics and significant selectivity for the imprint protein. This method seems rather versatile, since various vinyl functional monomers and different surface modified nanoparticles may be adopted according to the properties of protein to be imprinted. Further work aims at enhancing the imprinting efficiency with respect to both imprinting factor and specific rebinding capacity. This can be achieved by the rational design of the particle surface chemistry or the optimization of the prepolymerization recipes for a target protein. These studies are in progress and will be reported in the future.

Acknowledgments

The work was supported by the National Natural Science Foundation of China (No. 20574038) and the Natural Science Foundation of Tianjin (No. 09JCYBJC02900).

Appendix A. Supplementary data

Supplementary data associated with this article can be found, in the online version, at doi:10.1016/j.bios.2010.06.043.

References

Bereli, N., Andac, M., Baydemir, G., Say, R., Galaev, I.Y., Denizli, A., 2008. J. Chromatogr. A 1190, 18–26.
Bergmann, N.M., Peppas, N.A., 2008. Prog. Polym. Sci. 33, 271–288.
Bossi, A., Bonini, F., Turner, A.P.F., 2007. Biosens. Bioelectron. 22, 1131–1137.
Bossi, A., Piletsky, S.A., Piletska, E.V., Righetti, P.G., Turner, A.P.F., 2001. Anal. Chem. 73, 5281–5286.
Bourgeat-Lami, E., Lang, J., 1998. J. Colloid Interface Sci. 197, 293–308.
Cutivet, A., Schembri, C., Kovensky, J., Haupt, K., 2009. J. Am. Chem. Soc. 131, 14699–14702.
Fu, G.D., Zhao, J.P., Sun, Y.M., Kang, E.T., Neoh, K.G., 2007. Macromolecules 40, 2271–2275.
Gao, D.M., Zhang, Z.P., Wu, M.H., Xie, C.G., Guan, G.J., Wang, D.P., 2007. J. Am. Chem. Soc. 129, 7859–7866.
Hansen, D.E., 2007. Biomaterials 28, 4178–4191.
Haupt, K., Mosbach, K., 2000. Chem. Rev. 100, 2495–2504.
Hawkin, D.M., Stevenson, D., Reddy, S.M., 2005. Anal. Chim. Acta 542, 61–65.
Hoshino, Y., Kodama, T., Okahata, Y., Shea, K.J., 2008. J. Am. Chem. Soc. 130, 15242–15243.
Hu, X.B., Li, G.T., Huang, J., Zhang, D., Qiu, Y., 2007. Adv. Mater. 19, 4327–4332.
Hua, Z.D., Chen, Z.Y., Li, Y.Z., Zhao, M.P., 2008. Langmuir 24, 5773–5780.
Janiak, D.S., Kofinas, P., 2007. Anal. Bioanal. Chem. 389, 399–404.
Kan, X.W., Zhao, Q., Shao, D.L., Geng, Z.R., Wang, Z.L., Zhu, J.J., 2010. J. Phys. Chem. B 114, 3999–4004.
Kimhi, O., Bianco-Peled, H., 2007. Langmuir 23, 6329–6335.
Lee, K., Itharaju, R.R., Puleo, D.A., 2007. Acta Biomater. 3, 515–522.
Li, L., He, X.W., Chen, L.X., Zhang, Y.K., 2009. Chem. Asian J. 4, 286–293.
Li, Y., Yang, H.H., You, Q.H., Zhuang, Z.X., Wang, X.R., 2006. Anal. Chem. 78, 317–320.
Lin, H.Y., Ho, M.S., Lee, M.H., 2009. Biosens. Bioelectron. 25, 579–586.
Linares, A.V., Vandevelde, F., Pantigny, J., Falcimaigne-Cordin, A., Haupt, K., 2009. Adv. Funct. Mater. 19, 1299–1303.
Marty, J.D., Mauzac, M., 2005. Adv. Polym. Sci. 172, 1–35.
Nishino, H., Huang, C.S., Shea, K.J., 2006. Angew. Chem. Int. Ed. 45, 2392–2396.
Ou, S.H., Wu, M.C., Chou, T.C., Liu, C.C., 2004. Anal. Chim. Acta 504, 163–166.
Rachkov, A., Minoura, N., 2001. Biochim. Biophys. Acta 1544, 255–266.
Reimhult, K., Yoshimatsu, K., Risveden, K., Chen, S., Ye, L., Krozer, A., 2008. Biosens. Bioelectron. 23, 1908–1914.
Shiomi, T., Matsui, M., Mizukami, F., Sakaguchi, K., 2005. Biomaterials 26, 5564–5571.
Stöber, W., Fink, A., 1968. J. Colloid Interface Sci. 26, 62–69.
Tai, D.F., Jhang, M.H., Chen, G.Y., Wang, S.C., Lu, K.H., Lee, Y.D., Liu, H.T., 2010. Anal. Chem. 82, 2290–2293.
Turner, N.W., Jeans, C.W., Brain, K.R., Allender, C.J., Hlady, V., Britt, D.W., 2006. Biotechnol. Prog. 22, 1474–1489.
Wang, Y.T., Zhang, Z.Q., Jain, V., Yi, J.J., Mueller, S., Sokolov, J., Liu, Z.X., Levon, K., Rigas, B., Rafailovich, M.H., 2010. Sens. Actuat. B 146, 381–387.
Ye, L., Mosbach, K., 2008. Chem. Mater. 20, 859–868.
Zhang, M.S., Huang, J.R., Yu, P., Chen, X., 2010. Talanta 81, 162–166.
Zhao, Z., Wang, C.H., Guo, M.J., Shi, L.Q., Fan, Y.G., Long, L., Mi, H.F., 2006. FEBS Lett. 580, 2750–2754.
Zhou, W.H., Lu, C.H., Guo, X.C., Chen, F.R., Yang, H.H., Wang, X.R., 2010. J. Mater. Chem. 20, 880–883.